Indian Journal of Chemistry
Vol. 59A, July 2020, pp. 952-961

DFT investigation of pachypodol for exploring anti-oxidant action – Performance of B3LYP and M06-2X

D Jeevitha[a], K Sadasivam[a,]* & R Praveena[b]

[a]Department of Physics, Bannari Amman Institute of Technology (Autonomous), Sathyamangalam,

[b]Department of Chemistry, Bannari Amman Institute of Technology (Autonomous), Sathyamangalam, Erode-638 401, Tamil Nadu, India

Email: dftsada@gmail.com

Received 17 August 2019, Accepted 19 May 2020

Anti-oxidant mechanism of the pachypodol is computed with the aid of density functional theory (DFT) in the light of B3LYP (B3, Lee-Yang-Parr correlation function) and M06-2X (highly parameterized, exchange correlation function) using 6-311G(d,p) basis set in the Gaussian 09 software package. This investigation aims to prove the better reaction enthalpies among hydrogen atom transfer (HAT), sequential proton-loss electron-transfer (SPLET) and single electron transfer-proton transfer (SET-PT) in gas and solvent phases with both the level of theories (B3LYP and M06-2X). The result shows that the preferred anti-oxidant mechanism is found to be HAT in both gas and solvent phases. The analysis of bond dissociation enthalpy (BDE) has been carried out in gas and solvent phases. Molecular descriptors are analyzed and computed in the light of both the level of theories. The radical scavenging of pachypodol is well established with B3LYP theory, since it yields appreciable results with respect to BDE, IP and PDE than M06-2X level of theory. Fukui function of the compound is performed using both the level of theories and preferred electrophilic and nucleophilic sites of pachypodol are analyzed. The weak and strong intramolecular bonds are examined with the aid of NBO.

Keywords: Pachypodol, B3LYP, M06-2X, Anti-oxidant mechanism, Fukui function, NBO

Flavonoids are plant derived polyphenolic natural compounds exhibiting substantial scientific interest towards its radical scavenging ability. Flavonoids are evidenced through many researchers to possess biological activities such as anti-microbial, anti-inflammatory, anti-fungal and anti-oxidant activities. However, among them most interest is dedicated to their anti-oxidant activities.

Pachypodol (quercetin 3,7,3'-trimethyl ether or 4',5-Dihydroxy-3,3',7-trimethoxyflavone), a class of flavonoid, has been the subject of a numerous experimental studies dealing with its pharmacological activities such as anti-mutagenic activity[1], anti-emetic activity[2], inhibition of water-splitting enzyme[3], cytotoxic activity[4], anti-fungal activity[5], anti-poliovirus activity[6,7], anti-cancer activity[8], high anti-oxidant activity[9] anti-allergic and anti-inflammatory activities[10]. These defensive qualities make this compound very interesting and lead to the computational investigation on the radical scavenging ability.

Structure of pachypodol contains quercetin nucleus methoxylated at the hydroxyl groups in C-3, C-7, and C-3' positions of the ring. Structure and labelling of pachypodol is given in Fig. 1. Protective role and scavenging of free radicals of the compound are related with anti-oxidant activity. To explore the anti-oxidant related characteristics of pachypodol, DFT is implemented in the Gaussian 09W computational package[11]. B3LYP (hybrid exchange correlation functional) is the combination of a standard GGA with a part of HartreeFock exchange. Whilst M06-2X (hybrid meta-exchange correlation functional) has a GGA part, but also depends on the kinetic energy density, for which the results of two functional are compared here. M0-52X includes empirical corrections related to atomic dispersion

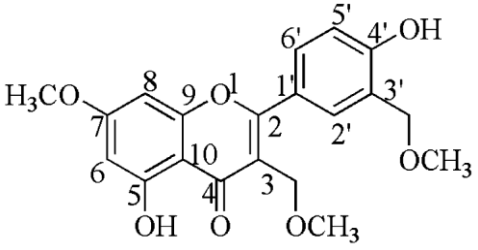

Fig. 1 — Structure and labeling of pachypodol compound.

with 56% of HF exchange whereas M0-62X is highly used to study thermochemistry, kinetics and non-covalent interactions of organic and inorganic species[12].

The three radical scavenging mechanisms HAT, SPLET and SET-PT help to get information regarding thermodynamically preferred mechanism. Further, electronic properties includes ionization potential (IP), electron affinity (EA), hardness (η), softness(S), electronegativity (χ), electrophilic index (ω) and BDE are evaluated and compared for pachypodol at both the level of theories. Natural bond orbital (NBO) method helps to identify strong and weak intramolecular hydrogen bonding.

Materials and Methods

Computational Methods

Optimization of neutral compound, radical, anion and cation are carried out employing both hybrid exchange correlation functional (B3LYP) and hybrid meta-exchange correlation functional (M06-2X) methods combined with the basis set 6-311G(d,p) as implemented in Gaussian 09 program. Electronic properties of pachypodol based on the value of E_o (orbital energy) and E_v (vertical energy) are computed with both the quantum methods. IP is the energy difference between the energy of the compound obtained from electron–transfer (radical cation) and the corresponding neutral compound.

$$IP_E = E_{cation} - E_n \quad \ldots(1)$$

EA is calculated as the energy difference between the neutral and anion species.

$$EA = E_n - E_{anion} \quad \ldots(2)$$

Based on these calculations the remaining electronic properties given as electronegativity (χ), hardness (η), softness (S) and electrophilic index (ω) are computed[13,14]

$$\mu \approx -\chi = -(IP + EA)/2 \quad \ldots(3)$$

$$\eta \approx (IP - EA)/2 \quad \ldots(4)$$

$$S = 1/(2\eta) \quad \ldots(5)$$

$$\omega = \mu^2/2\eta \quad \ldots(6)$$

In the literature of anti-oxidant behavior, phenolic anti-oxidants (ArOH) scavenge the free radicals by three main mechanisms[15,16] (i) A direct transfer of H-atom (HAT)[17] to the radical ($R^{\cdot}$) (ii) SPLET[18-20] mechanism includes a deprotonation precedes the electron transfer, which takes place once the anion ($ArO^{-\cdot}$) is formed. (iii) SET-PT involves the opposite procedure: phenolic anti-oxidant forms a radical cation by electron transfer that immediately forms phenoxyl radical by deprotonation.

HAT mechanism is related to the reactivity of an ArOH which is estimated by computing the O-H BDE where lower the BDE implies higher reactivity of pachypodol.

$$R^{\cdot} + ArOH \rightarrow ArO^{\cdot} + RH \quad \ldots(7)$$

$$BDE = H(ArO^{\cdot}) + H(H) - H(ArOH) \quad \ldots(8)$$

Where $H(ArO^{\cdot})$ refers the enthalpy of formation of pachypodol radical generated after H-abstraction; H(H) indicates the enthalpy of H-atom and H(ArOH) is the enthalpy of neutral molecule.

First step of second mechanism, SET-PT, is an electron-transfer reaction

$$ArOH + R^{\cdot} \rightarrow ArOH^{\cdot+} + e^{-} \quad \ldots(9)$$

This step is calculated by the value of IP

$$IP = H(ArOH^{\cdot+}) + H(e^{-}) - H(ArOH) \quad \ldots(10)$$

Second step is the deprotonation of $ArOH^{\cdot+}$

$$ArOH^{\cdot+} \rightarrow ArO^{\bullet} + H^{+} \quad \ldots(11)$$

The PDE is calculated as given

$$PDE = H(ArO^{\bullet}) + H(H^{+}) - H(ArOH^{\cdot+}) \quad \ldots(12)$$

where ,$H(H^{+})$ indicates the enthalpy of proton. Result of SET-PT mechanism is same as the result obtained from HAT mechanism.

First step in the SPLET mechanism is the anion radical (ArO^{-}) formation due to the proton loss

$$ArOH \rightarrow ArO^{-} + H^{+} \quad \ldots(13)$$

This step is related to PA and is calculated as follows

$$PA = H(ArO^{-}) + H(H^{+}) - H(ArOH) \quad \ldots(14)$$

The second step is the formation of $ArO^{\bullet}$ by the electron-transfer from ArO^{-}

$$ArO^{-} = ArO^{\bullet} - e^{-} \quad \ldots(15)$$

This step corresponds to the ETE which is determined as follows

$$ETE = H(ArO^{\bullet}) + H(e^{-}) - H(ArO^{-}) \quad \ldots(16)$$

where $H(ArO^{-})$ is the enthalpy of anion radical formed after the abstraction of proton (H^{+}). Result of SPLET mechanism resembles the result of HAT and SET-PT mechanism, because of the corresponding $ArO^{\bullet}$ radical formation and this study addresses the radical scavenging activity of pachypodol.

Results and Discussion

Bond dissociation enthalpy (BDE) in gas and solvent phases

Radical scavenging ability of a compound with multiple phenolic hydroxyl groups is determined by lowest O-H BDE magnitude. The computed BDE values in the gas phase are reported in Table 1. The most reactive system is identified through the H-atom transfer mechanism with the least BDE. It can be seen that pachypodol has the lowest BDE at 4'-OH than 5-OH at both level of theories.

In B3LYP method, BDE magnitude of 4'-OH at B-ring is significantly lower by 10.9 kcal/mol than 5-OH at A-ring. The same result is reflected in M06-2X, the only variation is the difference between the magnitudes of BDEs of 4'-OH and 5-OH as 9.47 kcal/mol. It reveals that H-atom abstraction is harder from A-ring than B-ring[21] and 4'-OH holds the lowest BDE of pachypodol which is due to the methoxylation substitution in ring A counterbalancing the contribution of catechol moiety in ring B. Moreover, least BDE result of 4'-OH belongs to B3LYP (74.24 kcal/mol) than M06-2X (77.98 kcal/mol).

The BDE computation is carried out at solvent phase with increasing order of polarity in benzene, ethanol and water to analyze interaction between solute and solvent which may considerably change the reactivity of studied molecule[22]. Solvent phase BDEs are in the same order of chemical reactivity as that of BDEs of gas phase. BDE magnitudes calculated using both the level of theories exhibit slight difference between gas and solvent phases as shown in Table 2 & Table 3.

However, in B3LYP, BDE values of gas and benzene phases exert a slight difference such as 0.83 kcal/mol for 4'-OH and 0.83 kcal/mol for 5-OH radical. Difference between the calculated BDEs of ethanol and gas phases are 2.25 kcal/mol for 4'-OH and 1.45 kcal/mol for 5-OH. Further, the variation between computed BDEs of gas and benzene phases with M06-2X presents 1.01 kcal/mol for 4'-OH and 2.47 kcal/mol for 5-OH radicals. The calculated BDEs of gas and solvent phases reveal that 4'-OH is the best candidate for radical scavenging activity since it possesses least BDE. Based on BDE values originating from gas and solvent phases, the order of radical scavenging ability with respect to the level of theory is

B3LYP > M06-2X

Also, Solvent effect does not alter the order of reactivity of pachypodol in both the level of theories.

Table 1 — Calculated bond dissociation enthalpy (BDE) values (kcal/mol) at 298.15 K in the gas phase for pachypodol at B3LYP/6-311G(d,p) and M06-2X/6-311G(d,p) level of theories

Radicals	Pachypodol	
	B3LYP/6-311G(d,p)	M06-2X/6-311G(d,p)
4'–OH	74.24	77.98
5-OH	85.14	87.45

Radical scavenging mechanism of pachypodol in gas and solvent phases

The computed values of anti-oxidant mechanisms (HAT, SPLET, SET-PT) of the pachypodol in both gas and solvent (water, benzene, ethanol) phases are reported in Table 2 & Table 3. The results obtained from all the three anti-oxidant mechanisms are

Table 2 — Calculated HAT, PDE, IP and PA (kcal/mol) for pachypodol at B3LYP/6-311G(d,p) level of theory

Medium (Without ZPC)	Nature of Species	HAT				SET-PT	SPLET
		BDE	IP	PDE	PA	IP+PDE	PA+ETE
Gas	Neutral	-	154.74	-	-	-	-
	4′-OH	81.83	-	242.25	341.12	396.99	397.74
	5-OH	93.75	-	254.17	348.80	408.91	409.66
Water	Neutral	-	127.35	-	-	-	-
	4′-OH	84.23	-	272.05	301.17	399.4	400.14
	5-OH	92.23	-	280.04	303.41	407.39	410.38
Benzene	Neutral	-	138.56	-	-	-	-
	4′-OH	82.66	-	259.26	319.28	397.82	398.56
	5-OH	92.92	-	269.52	324.74	408.08	408.83
Ethanol	Neutral	-	128.01	-	-	-	-
	4′-OH	84.08	-	271.23	302.38	399.24	399.99
	5-OH	92.30	-	279.44	304.90	407.45	408.20

Table 3 — Calculated HAT, PDE, IP and PA (kcal/mol) for pachypodol with M06-2X/6-311G(d,p) level of theory

Medium (Without ZPC)	Nature of Species	HAT				SET-PT	SPLET
		BDE	IP	PDE	PA	IP+PDE	PA+ETE
Gas	Neutral	-	164.61	-	-	-	-
	4′-OH	85.80	-	236.35	341.24	400.96	401.71
	5-OH	97.60	-	247.22	347.50	411.83	413.49
Water	Neutral	-	136.65	-	-	-	-
	4′-OH	88.62	-	267.13	299.80	403.78	404.53
	5-OH	98.11	-	274.46	302.18	411.11	414.04
Benzene	Neutral	-	147.98	-	-	-	-
	4′-OH	86.81	-	252.41	318.73	400.39	402.72
	5-OH	95.13	-	264.65	323.60	412.63	411.77
Ethanol	Neutral	-	137.04	-	-	-	-
	4′-OH	88.44	-	264.12	301.07	401.16	404.35
	5-OH	96.07	-	271.44	303.21	408.48	412.36

different which can provide an indication that the dominant mechanism for radical scavenging potency.

HAT mechanism is characterized by BDE which involves transferring of H-atoms from O-H groups of the compound to the free radical. BDE results obtained for 4'-OH radicalization are comparatively smaller than those calculated for 5-OH in both the quantum methods. The weakest O-H bond of the compound leads to provide high degree of anti-oxidant activity. It is evidenced from the Table 2 & Table 3, radicalization of 4'-OH leads to the most stable radical formation

Addition of PA with ETE results SPLET mechanism which are responsible for resolving the heterolytic BDE in which least magnitude has been observed for 4'-OH radical based on both the level of theories. Also, the lowest magnitude of PA is noted for radical 4'-OH. Since, proton transfer is easier from 4'-OH radical than 5-OH radical in pachypodol.

On analyzing SET-PT mechanism of both the quantum methods, it is concluded that IP and PDE are essential factors to identify the preferred site for electron and proton transfer from compound. Lower the magnitude of IP is the easier the electron transfer which account for first step of anti-oxidant mechanism in SET-PT. It is noted that the energy required for releasing H-atom (BDE) in both the level of theories are lesser compared to single electron transfer (IP). This is due to the fact that extended delocalization and conjugation of π-electrons. The PDE of 4'-OH is found to be minimum which is an essential factor for identifying the probable site for deprotonation obtained from second step of SET-PT. It is observed that 4'-OH is the desired site for O-H bond dissociation. The same behavior is evidenced from gas and solvent phase results that 4'-OH radical is the preferred site which is proved from HAT, SPLET and SET-PT mechanisms.

Analyzing the mechanisms, SPLET and SET-PT require more energy with respect to the HAT mechanism on both gas and solvent phases. Mechanism with least BDE, IP and PA magnitudes are considered to be the desirable mechanism[23,24] hence HAT is the preferred one on the basis of results obtained from gas and solvent phases in both the level of theories. In the light of computed magnitudes both in gas and solvent phases, it is observed that B3LYP level of theory produces lowest magnitude of BDE, PA and IP compared to M06-2X level. Klein et al[23] proved that the system with least magnitudes of enthalpies BDE, IP and PA establish the better anti-oxidant characteristics.

Molecular descriptors

Molecular descriptors are fundamental properties to characterize the chemical reactivity of the compounds[25,26]. Molecular descriptors of pachypodol are demonstrated in Table 4 with respect to E_v and E_o method. B3LYP method indicates that IP calculated from E_v is greater by 0.97 eV than E_o. EA calculated from E_v is lower than E_o by 1.01 eV. Further, the result of M06-2X refers that IP obtained from E_v has higher value than E_o by 0.09 eV. In terms of EA, E_v owns lesser value than E_o by 0.13 eV. IP is specified as the amount of energy needed to detach an electron

Table 4 — Molecular descriptors calculated from the E_v and E_o methods obtained at B3LYP/6-311G(d,p) and M06-2X/6-311G(d,p) level of theories (eV)

Molecular descriptors	B3LYP/6-311G(d,p) level of theory		M06-2X/6-311G(d,p) level of theory	
	E_v	E_o	E_v	E_o
IP	6.72	5.75	7.14	7.05
EA	0.53	1.54	0.49	0.62
H	3.09	2.10	3.32	3.26
S	1.54	1.05	1.66	1.63
X	3.62	3.64	3.81	3.88
Ω	2.31	3.15	2.18	2.30

from a molecule. Higher the IP value is the harder the electron removal[27,28].

IP computed from M06-2X is higher by 0.42 eV in E_v and 1.3 eV in E_o compared with B3LYP. At the same instant B3LYP provides higher magnitudes of EA in E_v and E_o by 0.04 eV and 0.92 eV, respectively than M06-2X methods. Electron affinity (EA) is defined as the amount of energy liberated when an electron is added to a neutral compound. Higher the EA values tend to higher the rate of electron removal[27,28]. Further, the computation of electronegativity (χ) also yields greater magnitude with M06-2X than B3LYP in both E_v and E_o methods. χ is calculated as the tendency to capture electrons in a chemical bond of the compound[26].

From obtained results, it is found that all the molecular descriptors have the lowest magnitudes with B3LYP except EA than M06-2X. Hassanzadeh et al.[29] investigated that the phenolic compounds with low magnitude of chemical descriptors exhibit the tendency of releasing the electron instead of attracting them. This behavior is the expected quality of the studied compound to exhibit the anti-oxidant characteristics[30]. In addition to magnitude of results, pachypodol prefers to act as electron donor rather than electron acceptor which is line with the results obtained from antioxidant mechanism analysis.

Frontier molecular orbitals

Highest occupied molecular orbital (HOMO) and lowest unoccupied molecular orbital (LUMO) are the important descriptors helping to exemplify the chemical reactivity and stability[31]. Further, FMO provides knowledge on the mechanism of anti-oxidant activity which in turn responsible for electron donating and accepting ability. The simulated FMOs are depicted in Fig. 2.

On analyzing the FMO with M06-2X and B3LYP methods, HOMO is outspread on the entire system but

Table 5 — Frontier molecular orbital (FMO) energies of pachypodol, computed with B3LYP/6-311G(d,p) and M06-2X/6-311G(d,p) quantum methods

FMO of pachypodol	B3LYP	M06-2X
$-\varepsilon_{HOMO}$/ eV	5.75	7.05
$-\varepsilon_{LUMO}$/ eV	1.54	0.62
Energy gap/ eV	4.21	6.43

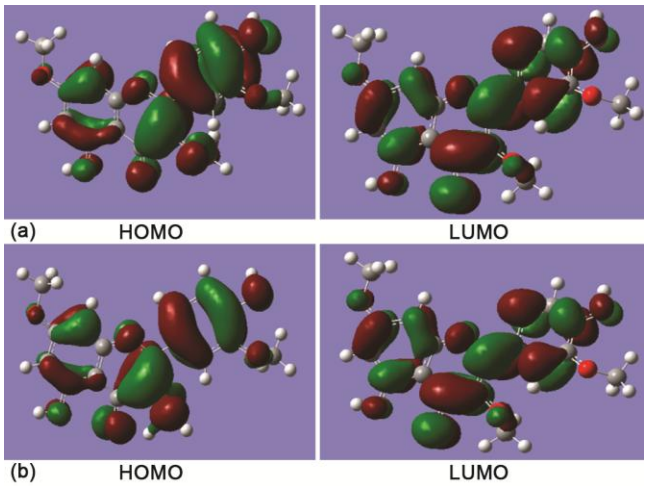

Fig. 2 — FMO of pachypodol at both quantum methods (a). B3LYP/6-311G(d,p) and (b). M06-2X/6-311G(d,p).

mainly localized on B-ring than A and C-rings, reveals that B-ring facilitates the electron donation. Charge distribution is found to be uniform throughout the system in the case of LUMO. An important structural feature which impacts over the localization of the electron in pachypodol is the presence of $–OCH_3$ units which has the influence over molecular hydrophobicity, electron donation and planarity. On other hand O-methyl substitution may cause steric hindrance, therefore decreasing anti-oxidant activity. Similarly ring B is particularly sensitive to substitution position. Therefore varying methylation on free hydroxyl groups in ring B improves anti-oxidant ability by altering coplanarity[32].

HOMO-LUMO energy gap describes the eventual charge transfer take place within the compound. From the Table 5, the computed energy gap of the pachypodol is 6.43 eV at M06-2X and 4.21 eV at B3LYP method. Hence, the energy gap of pachypodol acquired with B3LYP possesses least value than M06-2X. Lesser the energy gap easier the electron separation and stronger the anti-oxidant activity[33].

NBO analysis

The electronic structure of the pachypodol is examined with the aid of NBO method. NBO[34]

deals with the interaction takes place between the filled (bonding) orbitals and empty (anti-bonding) orbitals. The second order Fock matrix is accomplished to evaluate interaction of donor-acceptor. The stabilization energy E(2) is determined as

$$E_2 = \Delta E_{ij} = q_i = \frac{F(i,j)^2}{\epsilon_i - \epsilon_j} \quad \ldots(17)$$

where q_i refers donor orbital occupancy, E_i, and E_j indicate diagonal elements and $F_{i,j}$ means off diagonal Fock matrix elements. Larger the E(2) describes strong intramolecular interaction existing between electron-donor and acceptor. NBO analysis of pachypodol is computed with B3LYP and M06-2X methods.

Strong intramolecular hyperconjugative interactions takes place by the overlap of bonding (C–C), (C–O), (O–H), (O–H.....O) and anti–bonding (C–C), (C–O), (O–H) orbitals of flavone ring system at both the M06-2X and B3LYP models showed in Table 6 and Table 7. As expected, σ(C-C)→σ*(C-C) interaction is more intensive throughout the system such as, C15-C16→C17-C18 (23.26 kcal/mol), C5-C6→C2-C4 (35.76 kcal/mol) in M06-2X and C13-C14→C9-C10 (15.88 kcal/mol), C2-C4→C1-C3 (36.89 kcal/mol) in B3LYP method, which causes the stabilization of the whole system.

Table 6 — Second order perturbation theory analysis of Fock matrix for NBO analysis of pachypodol at M06-2X method

Donor (i)	Acceptor (j)	E(2) kcal/mol	E(j)-E(i) a.u.	F(i,j) a.u.
π(C1-C2)	π*(C1-C3)	5.65	1.40	0.080
	π*(C1-O8)	0.78	1.22	0.028
	π*(C2-H22)	1.88	1.29	0.044
	π*(O8-C9)	4.04	1.21	0.063
π(C1-C3)	π*(C1-C2)	5.62	1.41	0.080
	π*(O8-C9)	0.52	1.22	0.022
	σ*(C1-C3)	3.01	0.36	0.030
π(C1-O8)	π*(C1-C3)	1.22	1.65	0.040
σ(C2-C4)	σ*(C1-C3)	36.89	0.36	0.107
π(C2-H22)	π*(C1-C2)	1.41	1.21	0.037
	π*(C1-O8)	1.68	1.03	0.037
	π*(C2-C4)	1.62	1.23	0.040
π(C3-C5)	π*(C5-O23)	0.90	1.21	0.029
	π*(O23-H24)	1.92	1.25	0.044
π(C3-C11)	π*(C1-C2)	3.57	1.34	0.062
	π*(C5-C6)	2.54	1.37	0.053
	π*(C10-O36)	3.01	1.18	0.053
π(C4-C6)	π*(C2-H22)	3.02	1.29	0.056
	π*(C4-O25)	0.88	1.23	0.029
	π*(C5-O23)	4.14	1.22	0.064
π(C4-O25)	π*(C1-C2)	1.27	1.64	0.041
	π*(C2-C4)	1.23	1.65	0.040
π(C5-C6)	π*(C4-O25)	3.17	1.25	0.056
	π*(O23-H24)	0.61	1.28	0.025
σ(C5-C6)	σ*(C2-C4)	35.76	0.36	0.104
π(C5-O23)	π*(C3-C5)	1.18	1.62	0.039
π(C6-H7)	π*(C4-O25)	1.50	1.04	0.035
π(O8-C9)	π*(C1-C2)	2.23	1.63	0.054
	π*(C10-O36)	2.50	1.47	0.054
π(C9-C10)	π*(O8-C9)	0.82	1.26	0.029
σ(C9-C10)	σ*(C13-C14)	9.87	0.40	0.060
π(C10-O36)	π*(C3-C11)	1.18	1.49	0.038
	π*(C37-H39)	0.58	1.46	0.026
π(C13-C14)	π*(C9-C10)	2.55	1.44	0.054
σ(C13-C14)	π*(O8-C9)	1.09	0.72	0.027
	σ*(C15-C16)	25.14	0.35	0.085

(*Contd.*)

Table 6 — Second order perturbation theory analysis of Fock matrix for NBO analysis of pachypodol at M06-2X method (*Contd*.)

Donor (i)	Acceptor (j)	E(2) kcal/mol	E(j)-E(i) a.u.	F(i,j) a.u.
π(C14-C15)	π*(C15-H30)	1.76	1.28	0,042
π(C14-H21)	π*(C13-C14)	1.04	1.22	0.032
	π*(C15-H30)	0.85	1.08	0.027
σ(C15-C16)	σ*(C13-C14)	31.83	0.37	0.098
	σ*(C15-C16)	0.52	0.36	0.012
	σ*(C17-C18)	23.26	0.38	0.084
π(C15-H30)	π*(C14-C15)	1.28	1.24	0.036
π(C16-C17)	π*(C15-C16)	4.89	1.41	0.074
	π*(C15-H30)	2.52	1.28	0.051
	π*(C17-O31)	0.77	1.23	0.027
π(C17-C18)	π*(O31-C32)	1.81	1.16	0.041
σ(C17-C18)	σ*(C13-C14)	25.32	0.36	0.087
π(C17-O31)	π*(C17-C18)	1.59	1.62	0.045
π(C18-H41)	π*(C17-O31)	1.61	1.02	0.036
π(O19-H20)	π*(C16-C17)	4.92	1.43	0.076
π(O36-C37)	π*(C9-C10)	1.74	1.55	0.047
	σ*(C9-C10)	3.42	0.95	0.054
LP(1)O8	π*(C1-C3)	7.38	1.25	0.086
LP(2)O8	σ*(C1-C3)	36.23	0.46	0.122
LP(2)O12	π*(C3-C11)	24.43	0.83	0.129
	π*(C10-C11)	23.96	0.82	0.126
LP(1)O25	π*(C2-C4)	8.15	1.27	0.091
LP(2)O25	σ*(C2-C4)	40.78	0.45	0.128
LP(1)O36	π*(C18-H41)	0.53	1.15	0.022
LP(2)O36	π*(C37-H38)	6.81	0.88	0.070
	π*(C37-H40)	3.75	0.90	0.053
σ*(C1-C3)	σ*(C11-O12)	81.30	0.03	0.083
σ*(C13-C14)	σ*(C9-C10)	133.38	0.01	0.068
σ*(C15-C16)	σ*(C17-C18)	218.07	0.02	0.095

NBO analysis revealed that the magnitude of π(C-C)→π*(O-H) interaction is lesser than the π(O-H)→π*(C-C) interaction in both the level of theories (B3LYP, M06-2X). As mentioned, the interaction C5-C6→O23-H24 (0.61 kcal/mol) contributes lower energy than O19-H20→C16-C17 (4.92 kcal/mol) interaction in M06-2X also the same type of behavior is observed between C3-C5→O23-H24 (1.56 kcal/mol) and O19-H20→C16-C17 (4.34 kcal/mol) of B3LYP method. This denotes that the charge transfer from O–H towards carbon atoms of the ring leads to the conjugation of the system carry within the molecule. Further, more energetic contribution comes from oxygen lone pair of (O-H) to (C-C) anti-bonding orbital LP(2)O8→C1-C3 (36.23 kcal/mol) and LP(2)O8→C1-C3 (29.65 kcal/mol) in M06-2X and B3LYP, respectively. Enormous stabilization energy comes up with the interaction σ*(C15-C16)→σ*(C17-C18) (218.07 kcal/mol) with M06-2X method and σ*(C15-C16) →σ*(C13-C14) (288.46 kcal/mol) with B3LYP quantum method. These weak and strong interactions help to analyze the biological activity as well as radical scavenging activity of the system.

Fukui function analysis

Fukui functions helps to reveal both electrophilic and nucleophilic sites. The region pointed out in green color is preferable for nucleophilic attack which are more positive and meantime the region covered in color blue are more negative which is responsible for electrophilic attack [35,36]. While B3LYP method is taken into account, oxygen atom of 4'-OH, C13-C14, C16-C17 and on C15 of ring B exhibits higher electronegativity indicating electron deficiency there and only few negative regions are able to be seen on

Table 7 — Second order perturbation theory analysis of Fock matrix for NBO analysis of pachypodol at B3LYP method

Donor (i)	Acceptor (j)	E(2) kcal/mol	E(j)-E(i) a.u.	F(i,j) a.u.
π(C1-C2)	π*(C1-C3)	5.65	1.40	0.080
	σ*(C1-C3)	3.01	0.36	0.030
σ(C2-C4)	σ*(C1-C3)	36.89	0.36	0.107
π(C1-C2)	π*(C1-C3)	4.98	1.26	0.071
	π*(C1-O8)	0.65	1.06	0.023
	π*(C2-H22)	1.60	1.14	0.038
	π*(O8-C9)	3.56	1.05	0.055
π(C1-O8)	π*(C1-C2)	0.79	1.48	0.031
π(C2-C4)	π*(C1-C2)	3.36	1.27	0.058
	π*(C1-O8)	3.40	1.07	0.054
	π*(C2-H22)	1.77	1.15	0.040
σ(C2-C4)	σ*(C1-C3)	26.25	0.29	0.080
σ(C2-C4)	σ*(C1-C3)	26.25	0.29	0.080
	σ*(C5-C6)	12.09	0.29	0.054
π(C2-H22)	π*(C1-C2)	1.06	1.08	0.030
	π*(C1-O8)	1.40	0.88	0.031
	π*(C2-C4)	1.19	1.09	0.032
π(C3-C5)	π*(O23-H24)	1.56	1.09	0.037
π(C3-C11)	π*(C1-C2)	3.20	1.21	0.056
	π*(C10-C11)	0.88	1.10	0.028
	π*(C10-O36)	2.77	1.03	0.048
	π*(C11-O12)	1.81	1.26	0.043
π(C4-C6)	π*(C2-H22)	2.70	1.14	0.050
	π*(C6-H7)	1.47	1.13	0.036
	π*(O25-C26)	3.64	0.98	0.054
π(C4-O25)	π*(C1-C2)	1.16	1.47	0.037
π(C5-O23)	π*(C5-C6)	1.20	1.50	0.038
π(C6-H7)	π*(C2-C4)	4.25	1.09	0.061
	π*(C4-O25)	1.25	0.89	0.030
π(O8-C9)	π*(C1-C2)	1.95	1.46	0.048
	π*(C10-O36)	2.28	1.28	0.048
π(C9-C10)	π*(C10-O36)	1.37	1.12	0.035
	π*(O36-C37)	2.09	1.03	0.042
π(C9-C13)	π*(C1-O8)	3.58	1.02	0.054
π(C11-O12)	π*(C1-C3)	1.12	1.58	0.038
	π*(C10-C11)	1.79	1.48	0.047
σ(C11-O12)	σ*(C1-C3)	4.73	0.37	0.042
σ(C13-C14)	π*(O8-C9)	0.79	0.59	0.021
	σ*(C9-C10)	15.88	0.28	0.061
π(C13-C18)	π*(O8-C9)	1.98	1.02	0.040
	π*(C14-H21)	2.51	1.14	0.048
π(C14-H21)	π*(C13-C14)	0.76	1.08	0.026
	π*(C15-H30)	0.70	0.94	0.023
π(C15-C16)	π*(C14-C15	3.57	1.30	0.061
	π*(C14-H21)	2.14	1.17	0.045
π(C15-H30)	π*(C14-H21)	0.64	0.98	0.022
	π*(C16-C17)	4.19	1.06	0.060
π(C16-C17)	π*(O19-H20)	1.48	1.09	0.036
	π*(O31-C32)	0.69	0.99	0.024

(*Contd*.)

Table 7 — Second order perturbation theory analysis of Fock matrix for NBO analysis of pachypodol at B3LYP method (*Contd.*)

Donor (i)	Acceptor (j)	E(2) kcal/mol	E(j)-E(i) a.u.	F(i,j) a.u.
π(C16-O19)	π*(C14-C15)	1.23	1.51	0.039
π(C17-C18)	π*(C18-H41)	1.20	1.18	0.034
	π*(O31-C32)	1.82	0.99	0.038
π(C18-H41)	π*(C13-C14)	4.32	1.07	0.061
π(O19-H20)	π*(C16-C17)	4.34	1.28	0.067
π(O25-C26)	π*(C4-C6)	2.97	1.38	0.057
π(C26-H27)	π*(C4-O25)	0.52	0.91	0.019
LP(1)O8	π*(C1-C2)	0.83	1.10	0.027
LP(2)O8	π*(C1-C3)	29.65	0.36	0.098
	σ*(C9-C10)	28.04	0.38	0.092
LP(1)O12	π*(C3-C11)	2.24	1.12	0.045
LP(2)O12	π*(C37-H40)	0.57	0.66	0.018
LP(1)O25	π*(C26- H27)	0.68	0.92	0.022
LP(2)O31	σ*(C17-C18)	9.02	0.38	0.056
	π*(C32-H33)	5.84	0.74	0.060
σ*(C15-C16)	σ*(C 13-C14)	288.46	0.01	0.082
σ*(C17-C18)	π*(O31-C32)	0.82	0.26	0.031

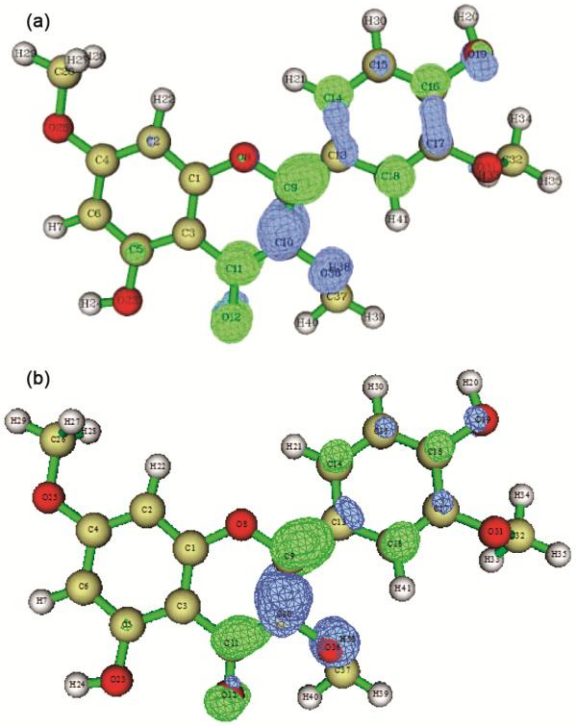

Fig. 3 — Electrophilic and nucleophilic sites of pachypodol from Fukui function obtained at (a) B3LYP/6-311G(d,p) and (b) M06-2X/6-311G(d,p) method.

ring C since it acts as electron donating region. Thus indicating that ring B is expected to be a preferable for electrophilic attack. So, the desirable site for an electrophilic attack is B-ring than A and C-rings. Carbonyl group (C=O) and C9-C13 are activated for nucleophilic attack as illustrated in Fig. 3a.When considering M06-2X quantum method, in Fig. 3(b),the region for nucleophilic attack appears to be the same as that of region shown in B3LYP method. But, very few regions are available for electrophilic attack in the ring B, like C13, C15, C17 and oxygen atom of 4'-OH group. It is clearly observed that in both the quantum methods, 4'-OH group is a good electrophile than 5-OH.

Conclusions

The anti-oxidant activity of the pachypodol is systematically performed in the framework of DFT with B3LYP/6-311G(d,p) and M06-2X/6-311G(d,p) level of theories. Anti-oxidant capability of the title compound has been explored with the aid of two levels of theories through three mechanisms (HAT, SPLET, SET-PT) in both gas and solvent phases (water, benzene, ethanol). Among the three mechanisms, HAT is found to be superior to other two mechanisms in the case of pachypodol. Also, three mechanisms predict that 4'-OH is the preferred deprotonation site. It is also observed that B3LYP level of theory yields lowest energy values of BDE, IP, PA and PDE of pachypodol in both phases (gas and solvent) in comparison with M06-2X level. The compound with least magnitudes of IP, PDE and PA is predominant in anti-oxidant activity[23]. On considering the HOMO-LUMO plot, the energy gap obtained with B3LYP method (4.21 eV) is lesser than M06-2X (6.43 eV) method. Lesser the energy gap more intensive the anti-oxidant activity of the studied

compound[32]. The results of obtained molecular descriptors are lower with B3LYP than M06-2X. Lower the chemical descriptor stronger the anti-oxidant action[29,30]. Further, NBO method analyzes the weak and strong interactions taking place within the pachypodol compound using both the quantum methods. Fukui function demonstrated the electrophilic and nucleophilic sites and 4'-OH is declared as a good electrophile than 5-OH which supports the BDE results.

References

1 Miyazawa M, Okuno Y, Nakamura S & Kosaka H, *J Agric Food Chem*, 48 (2000) 642.
2 Yang Y, Kinoshita K, Koyama K, Takahashi K, Tai T, Nunoura Y & Watanabe K, *Phytomedicine*, 6 (1999) 89.
3 Gonzalez-Vazquez R, Diaz B K, Aguilar M I, Diego N & Lotina-Hennsen B, *J Agric Food Chem*, 54 (2006) 1217.
4 Huong D T, Luong D V, Thao T T P & Sung T V, *Pharmazie*, 60 (2005) 627.
5 Citoglu G S, Sever B, Antus S, Baitz-Gacs E & Altanlar N, *Pharmaceut Biol*, 41 (2003) 483.
6 Ngadjui B T, Lontsi D, Ayafor J F & Sondengam B L, *Phytochemistry*, 28 (1989) 231.
7 Ngadjui B T, Ayafor J F & Lontsi D, *Fitoterapia*, 56 (1987) 340.
8 Ali H A, Azad Chowdhury A K, Rahman A K M, Borkowski T, Nahar L & Sarker S D, *Phytother Res*, 22 (2008) 1684.
9 Liu X, Yang D L, Liu J J, Xu K & Wu G H, *Chem Pap*, 68 (2014) 316.
10 Puripattanavong J & Tewtrakul S, *J Sci Technol*, 37 (2015) 37.
11 Frisch M J, Trucks G W, Schlegel H B, Scuseria G E, Robb M A, Chesseman J R, et al.(2009), *Gaussian 09, revision A.1-SMP, Wallingford, CT: Gaussian, Inc*.
12 Zhao Y & Truhlar D G, *Theor Chem Acc.*120 (2006) 215.
13 Denisova T G & Denisov E T, *Russ Chem Bull*, 57 (2008) 1858.
14 Laguerre M, Lecomte J & Villeneuve P, *Prog Lipid Res*, 46 (2007) 244.
15 Zhang H Y, Sun Y M & Wang X L, *Chemistry*, 9 (2003) 502.
16 Musialik M & Litwinienko G, *Org Lett*, 7 (2005) 4951.
17 Mayer J M & Rhile I J, *Biochim Biophys Acta*, 1655 (2004) 51.
18 Litwinienko G & Ingold K U, *J Org Chem*, 69 (2004) 5888.
19 Foti M C, Daquino C & Geraci C, *J Org Chem*, 69 (2004) 2309.
20 Galano A, Leon-Carmona J R & Alvarez-Idaboy J R, *J Phys Chem B*, 116 (2012) 7129.
21 Jeevitha D, Sadasivam K, Praveena R & Jayaprakasam R, *J Mol Struct*, 1120 (2016) 15.
22 Geerlings P, De Proft F & Langenaeker W, *Chem Rev*, 103 (2003) 1793.
23 Klein E, Lukes V & Ilcin M, *Chem Phys*, 336 (2007) 51.
24 Rimarcik J, Lukes V, Klein E & Ilcin M, *J Mol Struct*, 952 (2010) 25.
25 Parr R G & Pearson R G, *J Am Chem Soc*, 105 (1983) 7512.
26 Parr R G & Yang W. Density-Functional Theory of Atoms and Molecules, Oxford University Press, New York, 1989.
27 Foresman J B & Frisch E, Exploring Chemistry with Electronic Structure Methods, Second ed, Gaussian, Pittsburgh, PA, 1996.
28 Raj G, Advanced Inorganic Chemistry, Vol. 1. Krishna Prakashan Media, India, (2008).
29 Hassanzadeh K, Akhtari K, Hassanzadeh H, Zarei SA, Fakhraei N & Hassanzadeh K, *Food Chem*, 164 (2014) 251.
30 Pietta P G, *J Nat Prod*, 63 (2000) 1035.
31 Fukui K, *Science*, 218 (1982) 747.
32 Hidalgo M, Sánchez-Moreno C & de Pascual-Teresa S, *Food Chem*, 121 (2010) 691.
33 Cai W, Chen Y, Xie L, Zhang H & Hou C, *Eur Food Res Technol*, 238 (2014) 121.
34 Carpenter J E & Weinhold F, *J Mol Struct Thochem*, 169 (1988) 41.
35 Luque F J, Lopez J M & Orozco M, *Theor Chem Acc*, 103 (2000) 343.
36 Okulik N & Jubert A H, *Int Electron J Mol Des*, 4 (2005) 17